

RESEARCH ARTICLE | APRIL 21 2022

# Highly temperature-tolerant p-type carbon nanotube transistor doped with 1,4,5,8,9,11-hexaazatriphenylenehexacarbonitrile

Special Collection: [Advances in Low Dimensional and 2D Materials](#)

Yuki Matsunaga; Jun Hirotsu; Haruka Omachi



AIP Advances 12, 045322 (2022)

<https://doi.org/10.1063/5.0087868>

CHORUS

View  
OnlineExport  
Citation[CrossMark](#)

## Articles You May Be Interested In

A 1,4,5,8,9,11-hexaazatriphenylenehexacarbonitrile (HAT-CN) transport layer with high electron mobility for thick organic light-emitting diodes

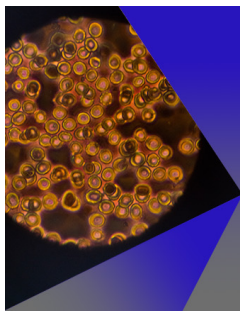
*AIP Advances* (May 2020)

Interlayer molecular diffusion and thermodynamic equilibrium in organic heterostructures on a metal electrode

*Journal of Applied Physics* (December 2011)

Refined drift-diffusion model for the simulation of charge transport across layer interfaces in organic semiconductor devices

*Journal of Applied Physics* (October 2018)



## AIP Advances

### Special Topic: Medical Applications of Nanoscience and Nanotechnology

**Submit Today!**

# Highly temperature-tolerant p-type carbon nanotube transistor doped with 1,4,5,8,9,11-hexaazatriphenylenehexacarbonitrile

Cite as: AIP Advances 12, 045322 (2022); doi: 10.1063/5.0087868

Submitted: 22 February 2022 • Accepted: 2 April 2022 •

Published Online: 21 April 2022



View Online



Export Citation



CrossMark

Yuki Matsunaga,<sup>1</sup> Jun Hirotsu,<sup>2,3,a)</sup> and Haruka Omachi<sup>1,4,a)</sup> 

## AFFILIATIONS

<sup>1</sup>Department of Chemistry, Graduate School of Science, Nagoya University, Furo-cho, Chikusa-ku, Nagoya 464-8602, Japan

<sup>2</sup>Department of Micro Engineering, Graduate School of Engineering, Kyoto University, Kyotodaigaku-Katsura C3, Nishikyo-ku, Kyoto 615-8540, Japan

<sup>3</sup>PRESTO, Japan Science and Technology Agency, 4-1-8 Honcho, Kawaguchi, Saitama 332-0012, Japan

<sup>4</sup>Research Center for Materials Science, Nagoya University, Furo-cho, Chikusa-ku, Nagoya 464-8602, Japan

**Note:** This paper is part of the AIP Advances Special Collection on Advances in Low Dimensional and 2D Materials.

**a) Authors to whom correspondence should be addressed:** [hirotani.jun.7v@kyoto-u.ac.jp](mailto:hirotani.jun.7v@kyoto-u.ac.jp) and [omachi@chem.nagoya-u.ac.jp](mailto:omachi@chem.nagoya-u.ac.jp)

## ABSTRACT

The development of chemical doping methods for carbon nanotubes (CNTs) is essential for various electronic applications. However, typical p-doping methods for CNT thin-film transistors (TFTs), using oxygen and water from the atmosphere, are quite sensitive to changes in the surrounding environment, and thus, their poor temperature tolerance is a critical problem during device fabrication. As a p-dopant for CNT-TFTs, we used 1,4,5,8,9,11-hexaazatriphenylenehexacarbonitrile (HATCN), which is a strong electron acceptor aromatic compound. The HATCN-doped CNT-TFTs exhibited p-type characteristics after exposure to a high-temperature environment of 200 °C, and prolonged heating did not degrade the p-doping performance of HATCN. In addition, stable p-type characteristics even under ambient conditions were obtained by encapsulating the surface of the device with a Parylene-Al<sub>2</sub>O<sub>3</sub> bilayer.

© 2022 Author(s). All article content, except where otherwise noted, is licensed under a Creative Commons Attribution (CC BY) license (<http://creativecommons.org/licenses/by/4.0/>). <https://doi.org/10.1063/5.0087868>

Carbon nanotubes (CNTs) have attracted considerable scientific and industrial attention due to their unique electronic,<sup>1,2</sup> mechanical,<sup>3,4</sup> and thermal<sup>5,6</sup> properties. In particular, they are used in thin-film transistors (TFTs)<sup>7-9</sup> as the channel material and in electronic devices.<sup>10,11</sup> The intrinsic ambipolar (both the hole and electron) charge-transport properties of CNTs remain a substantial problem in fabricating p-/n-type transistors, which are necessary for integrated circuits. In general, the carrier modulation of CNTs can be achieved by metal-semiconductor contacts at the source and drain electrodes<sup>12,13</sup> or chemical doping using electron-donor/accepter molecules in the channel region. Whereas metal-semiconductor contact engineering is effective for transistors with a short channel length,<sup>14</sup> chemical doping is suitable for long channel transistors because the carrier concentration can be controlled by the quantity of chemicals added. To date, multiple n-type<sup>15-19</sup> and p-type<sup>20-24</sup> dopants have been developed.

Many researchers have focused on reliable n-type dopants because most such dopants are readily oxidized by environmental changes. Recently, guanidino-functionalized aromatic compounds<sup>18</sup> and dimethyldihydrobenzimidazole<sup>19</sup> have been reported as air- and thermal-stable n-dopants that can be utilized during device fabrication.

Whereas researchers have developed many n-type dopants, the p-type doping of CNTs is usually conducted by physical adsorption of oxygen or water from air.<sup>20,21</sup> However, this approach has two problems: difficulty controlling the carrier concentration and low-temperature tolerance due to vaporization. CNT-TFTs applied in the aforementioned air-exposure process are susceptible to atmospheric humidity, and changes in the carrier concentration affect the device characteristics.<sup>20</sup> Instead of small molecules, organic oxidation reagents, such as 2,3,5,6-tetrafluoro-7,7,8,8-tetracyanoquinodimethane (F<sub>4</sub>-TCNQ)<sup>22</sup> and silver bis

(trifluoromethanesulfonyl)imide,<sup>24</sup> have also been used as p-dopants on CNTs. These oxidants have a high redox potential, which leads to highly degenerate states of CNTs and imparts difficulties in controlling the carrier density. In addition, high-temperature conditions readily degrade such organic molecules, and thus, one cannot use the dopants during device fabrication. Therefore, researchers would benefit from alternative dopants that do not have such drawbacks.

In this study, we found that 1,4,5,8,9,11-hexaazatriphenylene hexacarbonitrile (HATCN),<sup>25</sup> a chemical additive for the hole injection layers in organic light-emitting diodes,<sup>26–28</sup> is a promising candidate for the p-doping of CNTs. HATCN has a strong electron accepting ability originating from an electron-deficient *N*-heteroaromatic skeleton and the inductive effect of six electron-withdrawing cyano groups. We verified the doping ability of HATCN to CNT-TFT devices by the transfer characteristics, including the post-thermal treatment. We also demonstrated doped device operation under atmospheric conditions by depositing passivation films to prevent the permeation of oxygen.

Initially, semiconducting single-walled CNTs (s-SWCNTs) were separated for the fabrication of back-gate-type CNT-TFTs. The s-SWCNT dispersions were obtained by aqueous two-phase extraction based on our previous report.<sup>29</sup> SWCNTs (Meijo Nano Carbon, Meijo Arc SO type) (15 mg) were dispersed into 15 ml of 1 wt. % sodium cholate (Sigma-Aldrich, 99%) aqueous solution (aq.) with a bath sonicator (BM Equipment, Nanoruptor NR-350) for 16 h. The dispersion was then centrifuged at 276 000 g for 1 h with an ultracentrifuge (Hitachi Koki S52ST), and the upper 80% of the resultant dispersion was collected. The dispersion sample (2500  $\mu$ l) was added to a mixture containing 50 wt. % isomaltodextrin (Hayashibara Co., Ltd.) aq. (3000  $\mu$ l), 50 wt. % polyethylene glycol 6000 (Wako chemical) aq. (800  $\mu$ l), 10 wt. % sodium dodecyl sulfate (Sigma-Aldrich, 99%) aq. (100  $\mu$ l), 5 wt. % sodium glycocholate (TCI chemical) aq. (200  $\mu$ l), and deionized (DI) water (200  $\mu$ l). The quantity of sodium glycocholate aq. and DI water was optimized based on the target SWCNT dispersion. The resultant mixture settled for 15 min and was then centrifuged at 4000 g for 5 min with a microcentrifuge (Eppendorf MiniSpin plus) to

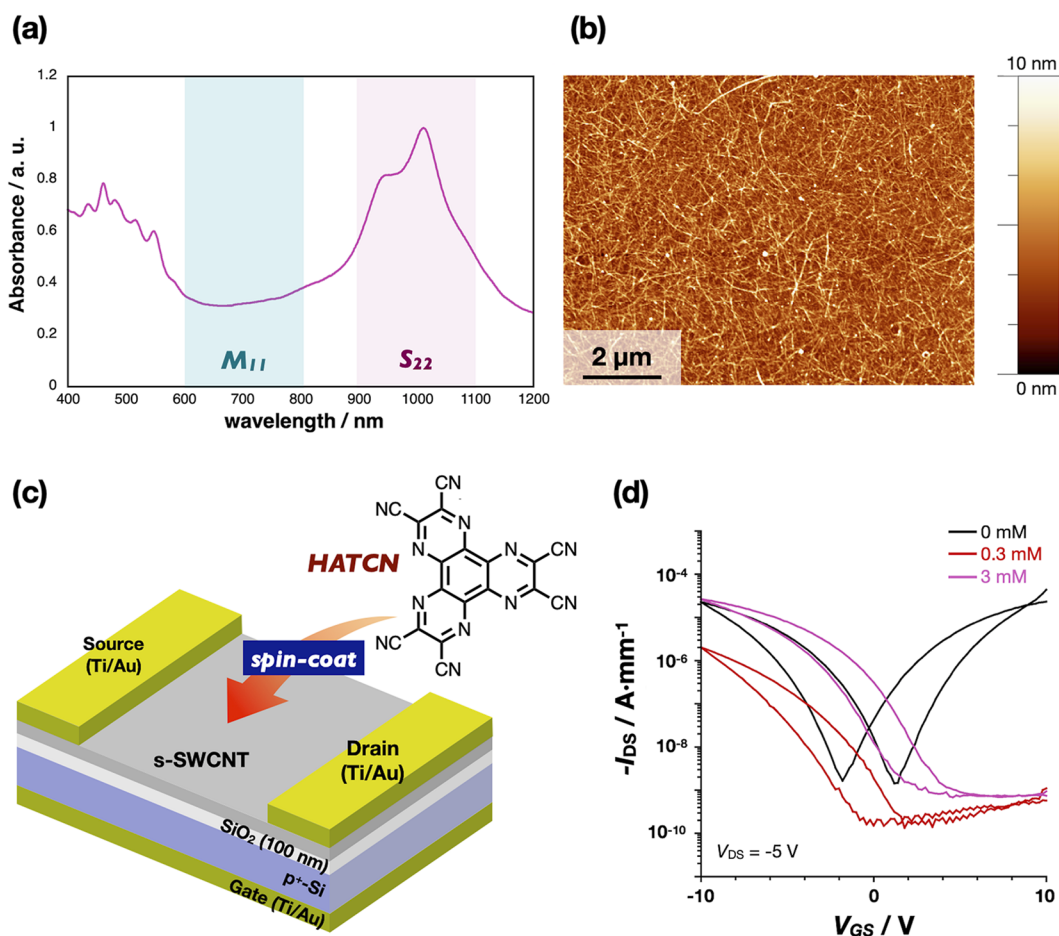


**FIG. 1.** (a) Absorption spectrum of a separated s-SWCNT dispersion normalized at the maximum peak intensity in the S<sub>22</sub> region. (b) Typical AFM image of an s-SWCNT thin film on an Si substrate. (c) Schematic of a HATCN-doped CNT-TFT ( $L = 100 \mu\text{m}$  and  $W = 100 \mu\text{m}$ ). (d) Transfer characteristics of CNT-TFTs doped with HATCN at various concentrations.

promote phase separation. The upper polyethylene glycol phase containing the desired s-SWCNTs was collected. The supernatant was evaluated using the absorption spectra measured with an ultraviolet–visible near-infrared spectrophotometer (JASCO V-770). Figure 1(a) shows the ultraviolet–visible absorption spectra of the separated semiconducting CNTs. The CNTs used in this study were 1.4–1.6 nm in diameter; we assigned the peaks at 600–800 and 900–1100 nm to metallic CNTs ( $M_{11}$ ) and semiconductor CNTs ( $S_{22}$ ), respectively.<sup>30</sup> The peak depression in the  $M_{11}$  region indicates that we selectively extracted the semiconducting CNTs. We estimate the purity of the semiconducting CNTs to be 99% based on previous reports.<sup>29</sup>

The heavily doped p-Si substrate, which had a 100 nm-thick thermally grown  $\text{SiO}_2$  layer and a back gate electrode, was functionalized with 3-aminopropyltriethoxysilane (TCI Chemical). The s-SWCNT dispersion (600  $\mu\text{l}$ ) was dropped onto the amine-terminated substrate to cover the entire surface. Afterward, the sample settled for 1 h, and it was then rinsed with DI water and 2-propanol. The substrate was immersed in hot DI water (90  $^\circ\text{C}$ ),

and the surfactants and impurities on the surface were removed. Atomic force microscopy (AFM) measurements were acquired with a Dimension FastScan instrument equipped with a Nanoscope V stage controller (Bruker). The AFM images of the fabricated s-SWCNT thin films indicate that the s-SWCNTs were uniformly deposited [Fig. 1(b)].

Figure 1(c) shows a schematic of the fabricated device. All electrodes were deposited via photolithography, electron beam deposition, and lift-off. To enhance the contact with the CNT thin film, 10-nm-thick titanium was deposited, followed by 100-nm-thick gold. Finally, the s-SWCNT thin film was patterned by photolithography and  $\text{O}_2$  plasma etching to afford channel lengths and widths of 100  $\mu\text{m}$  each. The fabricated devices were measured with a probe station connected to a semiconductor parameter analyzer (Keysight Technologies, B1500A) at room temperature in an  $\text{N}_2$  glovebox (oxygen concentration: 0.3 ppm and dew point:  $\sim -90$   $^\circ\text{C}$ ).

After placement in a glovebox, the fabricated CNT-TFTs were annealed at 150  $^\circ\text{C}$  for 5 min to remove the adsorbed oxygen and water from the substrate surface. The annealed devices were doped

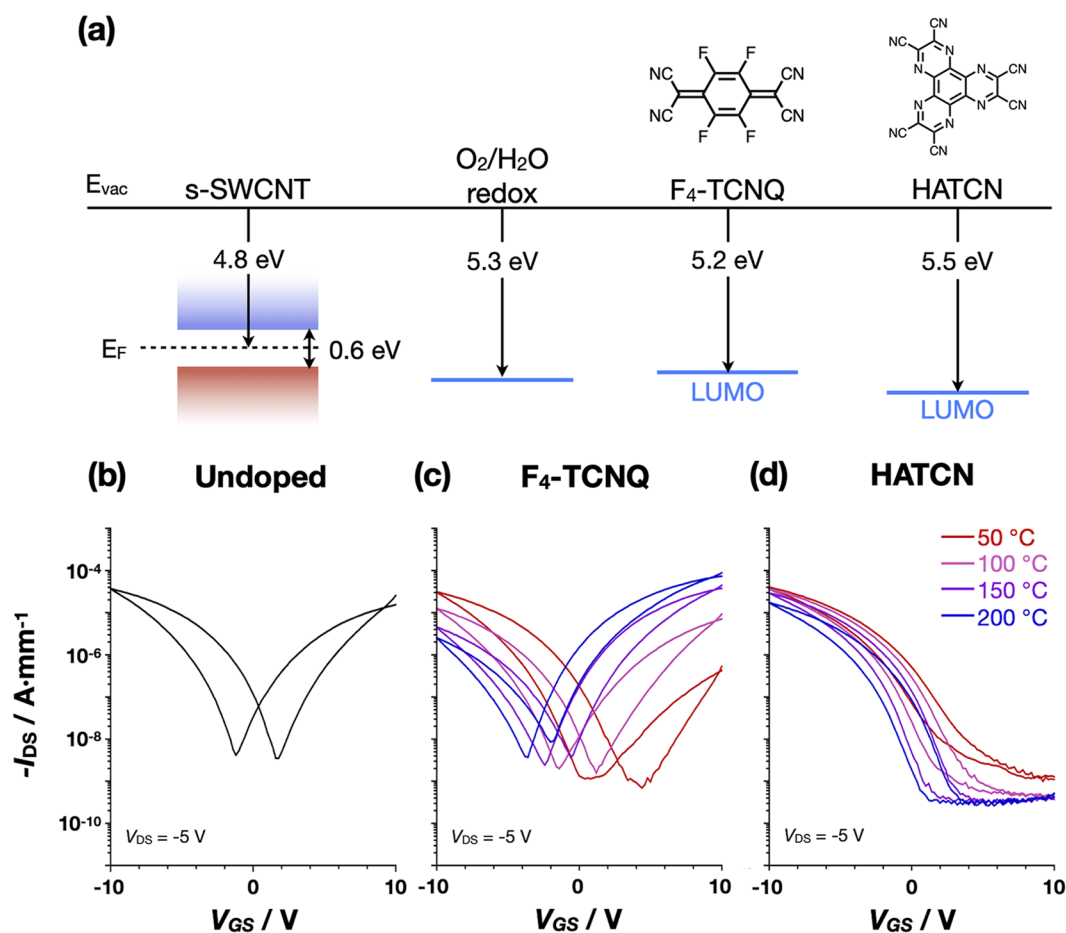


**FIG. 2.** (a) Energy level diagram for s-SWCNTs,  $\text{O}_2/\text{H}_2\text{O}$  redox,  $\text{F}_4\text{-TCNQ}$ , and HATCN. (b) Transfer characteristics of CNT-TFTs before doping. The transfer characteristics of CNT-TFTs doped with (c) 0.05 mM  $\text{F}_4\text{-TCNQ}$  and (d) 3 mM HATCN after heating at various temperatures are shown.

after the transfer characteristics had been measured and were confirmed to be ambipolar. A 200  $\mu\text{L}$  solution of HATCN in acetonitrile was dropped to cover the entire device and spin-coated at 5000 rpm (MIKASA Opticoat MS-B100) for 30 s. Figure 1(d) shows the transfer characteristics of the devices before doping (0 mM) and after spin-coating with 0.3 and 3 mM HATCN solutions, respectively. The device coated with 0.3 mM HATCN solution exhibited a p-type characteristic, where the current flows only when one applies a negative gate voltage. When we further increased the concentration of HATCN solution to 3 mM, the on-current density was  $26.6 \mu\text{A mm}^{-1}$  and the on-off ratio was  $3.92 \times 10^4$ . As we further increased the concentration of HATCN, the threshold voltage shifted in the positive direction. Therefore, we fixed the concentration of HATCN solution to 3 mM for further characterization of HATCN-doped devices.

Figure 2(a) shows the work function of SWCNTs and the lowest unoccupied molecular orbital (LUMO) of the reduction potential of oxygen,<sup>21</sup> F<sub>4</sub>-TCNQ,<sup>31</sup> and HATCN.<sup>32</sup> The Fermi energy of semiconducting SWCNTs was  $\sim 4.8 \text{ eV}$ ;<sup>33</sup> and we estimated the energy of the S<sub>11</sub> transitions, equivalent to the bandgap, to be 0.6 eV by using a Kataura plot<sup>30</sup> based on the diameter of the CNTs used in this work. Because the reduction potential of oxygen and the LUMO level of F<sub>4</sub>-TCNQ are lower than the Fermi energy of SWCNTs, they act as electron acceptors to induce hole injection into the SWCNTs. HATCN had a lower LUMO level than F<sub>4</sub>-TCNQ, and the band diagram indicates that HATCN is useful as a p-dopant.

To compare the CNT-TFTs doped with these three types of p-dopants, we conducted the measurements in a glove box to eliminate the influence of oxygen and water molecules in ambient air. Figure 2(b) shows the transfer characteristics of the CNT-TFTs after baking at 150 °C for 5 min under an inert N<sub>2</sub> atmosphere. The devices exhibited bipolar behavior, not the p-type behavior that is characteristic of doping with oxygen and water molecules. However, we did not completely eliminate the hysteresis. It seems

likely that simple annealing could not completely remove the surface adsorbed water, on which the charging and discharging were induced.<sup>20,35</sup>

Figures 2(c) and 2(d) show the transfer characteristics of CNT-TFTs spin-coated with 0.05 mM F<sub>4</sub>-TCNQ or 3 mM HATCN, respectively, after heating at 50, 100, 150, and 200 °C for 5 min. The device treated with F<sub>4</sub>-TCNQ solution showed slight p-type character after heating at 50 °C. However, when we heated the device to 100 °C, it changed back to the ambipolar property because the sublimation of F<sub>4</sub>-TCNQ starts at  $\sim 85 \text{ °C}$ .<sup>34</sup> We confirmed stable p-type characteristics in the case of devices spin-coated with HATCN solution even after heating to 200 °C. It is proposed that the high-temperature tolerance of HATCN is due to its larger molecular weight compared with F<sub>4</sub>-TCNQ.<sup>36</sup> As the heating temperature increased, the on-current decreased and the threshold voltage shifted to the negative direction. This is probably caused by incorporation of water in acetonitrile in which HATCN was dissolved, and the evaporation caused by heating changed the transfer characteristics.

We further investigated the time-dependent tolerance of HATCN at 200 °C. We doped the fabricated CNT-TFTs in the same manner as in Fig. 1(d), and we measured their transfer characteristics after heating at 200 °C for 5 min, 1 h, 8 h, 24 h, and 72 h. We obtained stable p-type behavior even after heating the substrate at 200 °C for up to 72 h [Fig. 3(a)]. Figure 3(b) shows a graph of on-current density and threshold voltage vs heating time. Both the on-current and threshold voltage increased as the heating time increased, but they became saturated after 72 h of heating. The results also indicate the improvement of the transconductance and carrier mobility with prolonged heating.

Finally, we measured CNT-TFTs doped with HATCN under aerobic conditions. We passivated the top surface of the device [Fig. 4(a)] to prevent the permeation of oxygen and water from air to measure the desired characteristics as affected by HATCN only.

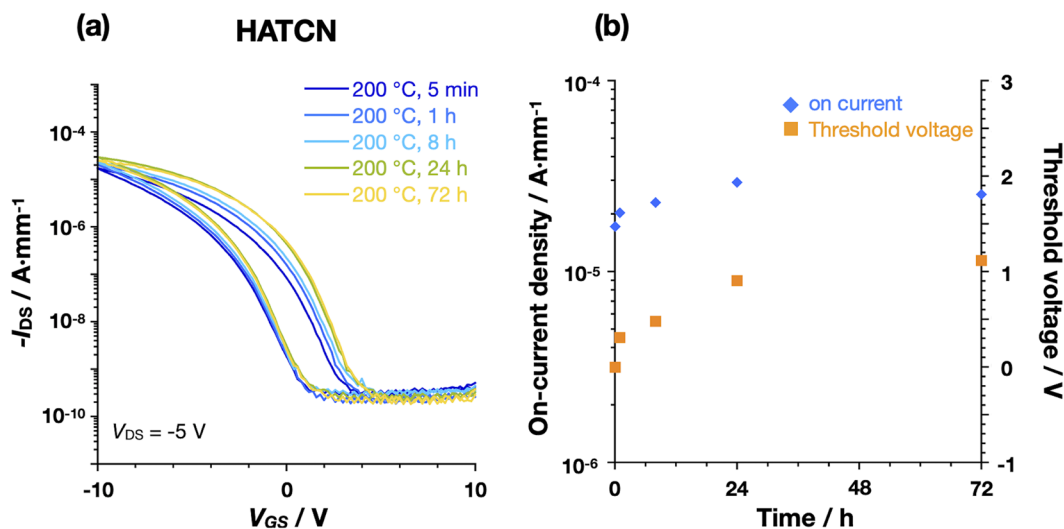
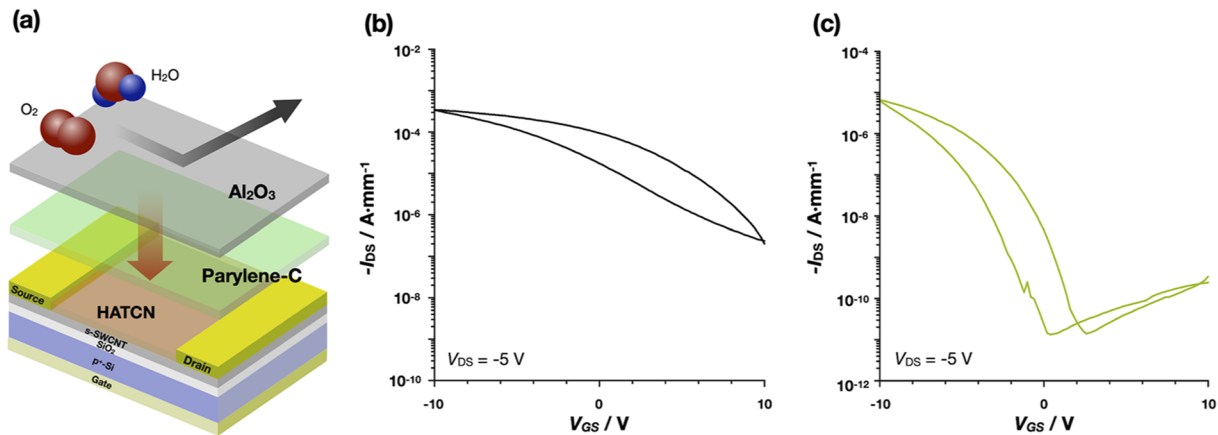


FIG. 3. (a) Transfer characteristics of CNT-TFTs doped with 3 mM HATCN at various heating times. (b) On-current change (blue) and threshold voltage change (orange) as a function of heating time.



**FIG. 4.** (a) Schematic of a doped CNT-TFT passivated with a Parylene- $\text{Al}_2\text{O}_3$  bilayer. The transfer characteristics of doped CNT-TFTs (b) without and (c) with passivation are shown.

When we directly deposited  $\text{Al}_2\text{O}_3$  (commonly used as a passivation layer for CNT-TFTs<sup>37</sup>) on the device, HATCN on the CNT channel could be removed under high-vacuum conditions of an atomic layer deposition system. After extensive trial-and-error, we found that pre-coating with a polymer film suppressed the sublimation of HATCN molecules. We deposited Parylene-C with a thickness of 300 nm at room temperature with a Parylene coater (SCS Labcoater 2 PDS 2010) and then continuously deposited  $\text{Al}_2\text{O}_3$  with atomic layer deposition equipment (Cambridge NanoTech, Savannah 100) at 200 °C at a thickness of 50 nm. Although the transfer characteristics of a HATCN-doped CNT-TFT without passivation layers exhibited relatively large on-current density, we observed a decrease in the on-off ratio and a predominantly on state, compared with the measurement in inert  $\text{N}_2$  atmospheric conditions due to the absorption of the environmental water and oxygen [Fig. 4(b)]. Figure 4(c) shows the transfer characteristics of the encapsulated devices in air. The device exhibited stable p-type behavior without the influence of small molecules.

In conclusion, we revealed that HATCN is a valuable p-dopant for CNT-TFTs that exhibit excellent temperature tolerance. We readily doped the devices by straightforward spin-coating with HATCN solution. The HATCN-doped CNT-TFTs exhibited stable p-type character even after high-temperature treatment at 200 °C for 72 h, a remarkable temperature tolerance compared with conventional p-dopants, such as oxygen and  $\text{F}_4\text{-TCNQ}$ . Furthermore, the doped devices demonstrated stable p-type operation by encapsulation with Parylene-C and  $\text{Al}_2\text{O}_3$ , preventing the influence of oxygen from the surrounding environment. Such p-dopants with excellent high-temperature tolerance will be developed into low-consumption complementary metal-oxide-semiconductor circuits and flexible thermoelectric device applications of CNTs with a precisely controlled doping concentration by combining them with previously reported n-type dopants.

This work received financial support from the JST CREST (Grant No. 19203618), the PRESTO (Grant No. JPMJPR20B6), and the JSPS Grant-in-Aid for Scientific Research (Grant Nos. JP19H02168 and 20KK0087).

## AUTHOR DECLARATIONS

### Conflict of Interest

The authors have no conflicts to disclose.

### DATA AVAILABILITY

The data that support the findings of this study are available from the corresponding authors upon reasonable request.

## REFERENCES

- A. Javey, J. Guo, Q. Wang, M. Lundstrom, and H. Dai, *Nature* **424**, 654 (2003).
- A. D. Franklin, M. Luisier, S.-J. Han, G. Tulevski, C. M. Breslin, L. Gignac, M. S. Lundstrom, and W. Haensch, *Nano Lett.* **12**, 758 (2012).
- M. M. J. Treacy, T. W. Ebbesen, and J. M. Gibson, *Nature* **381**, 678 (1996).
- D. Bozovic, M. Bockrath, J. H. Hafner, C. M. Lieber, H. Park, and M. Tinkham, *Phys. Rev. B* **67**, 033407 (2003).
- C. Yu, L. Shi, Z. Yao, D. Li, and A. Majumdar, *Nano Lett.* **5**, 1842 (2005).
- B. A. MacLeod, N. J. Stanton, I. E. Gould, D. Wesenberg, R. Ihly, Z. R. Owczarczyk, K. E. Hurst, C. S. Fewox, C. N. Folmar, K. Holman Hughes, B. L. Zink, J. L. Blackburn, and A. J. Ferguson, *Energy Environ. Sci.* **10**, 2168 (2017).
- Q. Cao and J. A. Rogers, *Adv. Mater.* **21**, 29 (2009).
- Y. Yang, L. Ding, J. Han, Z. Zhang, and L.-M. Peng, *ACS Nano* **11**, 4124 (2017).
- D.-M. Sun, M. Y. Timmermans, A. Kaskela, A. G. Nasibulin, S. Kishimoto, T. Mizutani, E. I. Kauppinen, and Y. Ohno, *Nat. Commun.* **4**, 2302 (2013).
- L. Xiang, H. Zhang, Y. Hu, and L.-M. Peng, *J. Mater. Chem. C* **6**, 7714 (2018).
- G. Hills, C. Lau, A. Wright, S. Fuller, M. D. Bishop, T. Srimani, P. Kanhaiya, R. Ho, A. Amer, Y. Stein, D. Murphy, Arvind, A. Chandrakasan, and M. M. Shulaker, *Nature* **572**, 595 (2019).
- D. Shahjerdi, A. D. Franklin, S. Oida, J. A. Ott, G. S. Tulevski, and W. Haensch, *ACS Nano* **7**, 8303 (2013).
- Y. Noshu, Y. Ohno, S. Kishimoto, and T. Mizutani, *Nanotechnology* **17**, 3412 (2006).
- J. Tang, D. Farmer, S. Bangsaruntip, K.-C. Chiu, B. Kumar, and S.-J. Han, in International Symposium on VLSI Technology, Systems and Application, April 2017.
- V. Derycke, R. Martel, J. Appenzeller, and P. Avouris, *Appl. Phys. Lett.* **80**, 2773 (2002).

- <sup>16</sup>S. M. Kim, J. H. Jang, K. K. Kim, H. K. Park, J. J. Bae, W. J. Yu, I. H. Lee, G. Kim, D. D. Loc, U. J. Kim, E.-H. Lee, H.-J. Shin, J.-Y. Choi, and Y. H. Lee, *J. Am. Chem. Soc.* **131**, 327 (2009).
- <sup>17</sup>B. R. Kang, W. J. Yu, K. K. Kim, H. K. Park, S. M. Kim, Y. Park, G. Kim, H.-J. Shin, U. J. Kim, E.-H. Lee, J.-Y. Choi, and Y. H. Lee, *Adv. Funct. Mater.* **19**, 2553 (2009).
- <sup>18</sup>S. Schneider, M. Brohmann, R. Lorenz, Y. J. Hofstetter, M. Rother, E. Sauter, M. Zharnikov, Y. Vaynzof, H.-J. Himmel, and J. Zaumseil, *ACS Nano* **12**, 5895 (2018).
- <sup>19</sup>H. Wang, P. Wei, Y. Li, J. Han, H. R. Lee, B. D. Naab, N. Liu, C. Wang, E. Adjanto, B. C.-K. Tee, S. Morishita, Q. Li, Y. Gao, Y. Cui, and Z. Bao, *Proc. Natl. Acad. Sci. U. S. A.* **111**, 4776 (2014).
- <sup>20</sup>W. Kim, A. Javey, O. Vermesh, Q. Wang, Y. Li, and H. Dai, *Nano Lett.* **3**, 193 (2003).
- <sup>21</sup>C. M. Aguirre, P. L. Levesque, M. Paillet, F. Lapointe, B. C. St-Antoine, P. Desjardins, and R. Martel, *Adv. Mater.* **21**, 3087 (2009).
- <sup>22</sup>T. Takenobu, T. Kanbara, N. Akima, T. Takahashi, M. Shiraishi, K. Tsukagoshi, H. Kataura, Y. Aoyagi, and Y. Iwasa, *Adv. Mater.* **17**, 2430 (2005).
- <sup>23</sup>K. K. Kim, J. J. Bae, H. K. Park, S. M. Kim, H.-Z. Geng, K. A. Park, H.-J. Shin, S.-M. Yoon, A. Benayad, J.-Y. Choi, and Y. H. Lee, *J. Am. Chem. Soc.* **130**, 12757 (2008).
- <sup>24</sup>S. M. Kim, Y. W. Jo, K. K. Kim, D. L. Duong, H.-J. Shin, J. H. Han, J.-Y. Choi, J. Kong, and Y. H. Lee, *ACS Nano* **4**, 6998 (2010).
- <sup>25</sup>K. Kanakarajan and A. W. Czarnik, *J. Org. Chem.* **51**, 5241 (1986).
- <sup>26</sup>S.-H. Son, O.-H. Kim, S.-H. Yoon, K.-K. Kim, Y.-G. Lee, and J.-S. Bae, U.S. patent 6,720,573 B2 (10 March 2004).
- <sup>27</sup>L. S. Liao, W. K. Slusarek, T. K. Hatwar, M. L. Ricks, and D. L. Comfort, *Adv. Mater.* **20**, 324 (2008).
- <sup>28</sup>S. Ohisa, Y.-J. Pu, S. Takahashi, T. Chiba, and J. Kido, *Polym. J.* **49**, 149 (2017).
- <sup>29</sup>H. Omachi, T. Komuro, K. Matsumoto, M. Nakajima, H. Watanabe, J. Hirotsu, Y. Ohno, and H. Shinohara, *Appl. Phys. Express* **12**, 097003 (2019).
- <sup>30</sup>H. Kataura, Y. Kumazawa, Y. Maniwa, I. Umezumi, S. Suzuki, Y. Ohtsuka, and Y. Achiba, *Synth. Met.* **103**, 2555 (1999).
- <sup>31</sup>W. Gao and A. Kahn, *Appl. Phys. Lett.* **79**, 4040 (2001).
- <sup>32</sup>D. P.-K. Tsang, T. Matsushima, and C. Adachi, *Sci. Rep.* **6**, 22463 (2016).
- <sup>33</sup>S. Suzuki, C. Bower, Y. Watanabe, and O. Zhou, *Appl. Phys. Lett.* **76**, 4007 (2000).
- <sup>34</sup>J. Drechsel, M. Pfeiffer, X. Zhou, A. Nollau, and K. Leo, *Synth. Met.* **127**, 201 (2002).
- <sup>35</sup>A. D. Franklin, G. S. Tulevski, S.-J. Han, D. Shahrjerdi, Q. Cao, H.-Y. Chen, H.-S. P. Wong, and W. Haensch, *ACS Nano* **6**(2), 1109 (2012).
- <sup>36</sup>P. Frank, T. Djuric, M. Koini, I. Salzmann, R. Rieger, K. Müllen, R. Resel, N. Koch, and A. Winkler, *J. Phys. Chem. C* **114**, 6650 (2010).
- <sup>37</sup>S. Won Lee, D. Suh, S. Young Lee, and Y. Hee Lee, *Appl. Phys. Lett.* **104**, 163506 (2014).